

# Asteroseismology of the $\beta$ Cephei star $\nu$ Eridani: massive exploration of standard and non-standard stellar models to fit the oscillation data

M. Ausseloos,<sup>1\*</sup> R. Scuflaire,<sup>2</sup> A. Thoul<sup>2</sup> and C. Aerts<sup>1,3</sup>

<sup>1</sup>*Institute of Astronomy, Catholic University of Leuven, Celestijnenlaan 200B, B-3001 Leuven, Belgium*

<sup>2</sup>*Institut d'Astrophysique et de Géophysique de Liège, Université de Liège, allée du Six Août 17, 4000 Liège, Belgium*

<sup>3</sup>*Department of Astrophysics, University of Nijmegen, PO Box 9010, 6500 GL Nijmegen, the Netherlands*

Accepted 2004 August 16. Received 2004 August 13; in original form 2004 June 10

## ABSTRACT

We present the results of a detailed seismic modelling of the  $\beta$  Cephei star  $\nu$  Eridani with the Liège evolution and pulsation codes. We selected four clearly detected, well-identified and independent pulsation modes from the frequency spectrum obtained from a recent five-month multisite, multitechnique campaign, while previous modelling work only took into account three frequencies. We show by means of a massive exploration of the parameter space that no standard stellar model both matches and excites these four observed modes, in contrast to the conclusion reached when considering only three frequencies. Therefore, we have considered stellar models with different metal mixtures and different initial hydrogen abundance values. We show that an increase in the relative number fraction of iron throughout the whole star or a large decrease in the initial hydrogen abundance make the stellar models matching the four selected modes satisfy all observational constraints and we provide the general properties of the best such physical models.

**Key words:** stars: early-type – stars: individual:  $\nu$  Eridani – stars: oscillations – stars: variables: other.

## 1 INTRODUCTION

The observation of many different types of stars of different ages has led to a stellar evolution theory that is reasonably well established in a global sense. However, our knowledge of specific aspects of the physics, such as convection, internal rotation, mixing, etc., is rather limited. The hope is that asteroseismology will lead to significant contributions in this context in line with the implications that helioseismology had for detailed stellar structure models of the Sun (see, for example, Christensen-Dalsgaard 2002, for a review). In this paper, we apply seismic techniques to a massive main-sequence B-type star exhibiting low-order pressure and gravity modes with periods of the order of a few hours. Such stars are termed  $\beta$  Cephei stars. Handler et al. (2004, hereafter Paper I) have already given a brief overview of the problems and prospects for asteroseismology of the  $\beta$  Cephei stars, which are massive near-main-sequence stars of spectral type between B0 and B2. Such stars have well-developed convective cores, which would be good laboratories to derive convective properties if we could probe them. As for rotation, it turns out that the  $\beta$  Cephei stars are slow to moderate rotators, with  $v \sin i$  well below 20 per cent of the break-up velocity for almost all members (Aerts & De Cat 2003).

Previous seismic studies of  $\beta$  Cephei stars (for an overview, see Aerts et al. 2004, hereafter Paper II) were hampered by the relatively limited number of independent frequencies and the unknown mode identification of some of them. Therefore, Handler & Aerts (2002) set up a five-month multisite campaign for the  $\beta$  Cephei star  $\nu$  Eridani ( $\nu$  Eri, HD 29248, B2III). This resulted in more than 600 h of mmag-level multicolour photometric data and about 2500 high-temporal and high-resolution spectra. A period analysis revealed eight independent pulsation frequencies between 5–8 cycle  $d^{-1}$  ( $cd^{-1}$ ) in the photometric data (Paper I) and seven in the spectroscopic data (Paper II). These observed frequency spectra are graphically depicted in Fig. 1. De Ridder et al. (2004, hereafter Paper III) performed an extended frequency analysis on different line-profile diagnostics revealing an additional significant frequency and four additional candidates in the spectroscopic data. In Paper III, mode identification was also performed and all observational results of the multisite campaign were summarized.

The results presented in Paper III constitute the starting point of our thorough basic seismic modelling of  $\nu$  Eri, in which we try to match stellar models to the obtained oscillation data. The goal of this paper is threefold. First, we want to examine to what extent the observational constraints put limits on stellar models. More specifically, we derive the sets of stellar parameter values that correspond to standard stellar models which explain well  $\nu$  Eri's pulsational behaviour and look at whether these sets are confined to

\*E-mail: mario@ster.kuleuven.ac.be

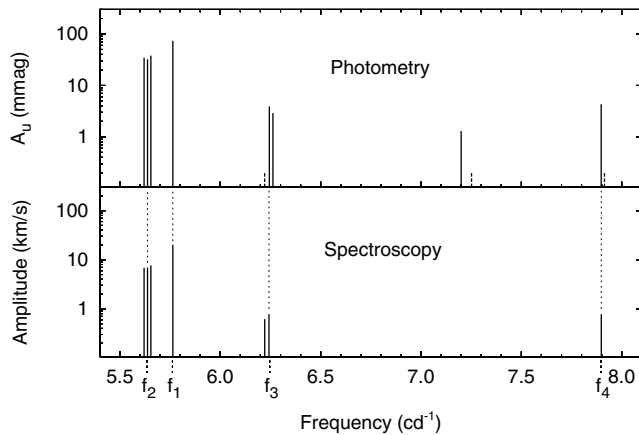


**Figure 1.** Photometric (upper panel) and spectroscopic (lower panel) observed frequency spectra in the range  $[5.4, 8.1] \text{ cd}^{-1}$ . Confirmed frequencies are indicated by solid lines while suspected frequencies are denoted with a thick dashed line with an arbitrary, small amplitude. The four frequencies on which the seismic modelling is based are labelled  $f_1$ ,  $f_2$ ,  $f_3$  and  $f_4$ . Their corresponding peaks in the two panels are connected by a thin, dotted line.

a small region in stellar parameter space or spread out over different regions. Secondly, we investigate the influence of the number of observed frequencies on the results of the seismic analysis. Thirdly, we compare the results of the seismic modelling of  $\nu$  Eri carried out recently by Pamyatnykh, Handler & Dziembowski (2004) on the basis of the Warsaw–New Jersey evolution and oscillation codes, which are entirely independent of the codes used by us, with our results.

The paper is organized as follows. In Section 2 we begin with a description of the calculated grid of standard stellar models and the observational constraints derived for  $\nu$  Eri. In the following sections we impose the matching of respectively two (Section 3), three (Section 4) and four (Section 5) observed frequencies to standard stellar models. We also consider non-standard stellar models in Section 6 and end with a discussion in Section 7.

## 2 STARTING POINT OF THE MODELLING

We have calculated an extensive grid of standard stellar models using the evolutionary code CLES (Code Liégeois d’Évolution Stellaire). We used the opacities derived from the OPAL code (Iglesias & Rogers 1996), completed with the Alexander & Ferguson (1994) opacities below  $\log T = 3.95$ . We adopted the CEFF equation of state (Christensen-Dalsgaard & Däppen 1992) and the standard heavy-element mixture (Grevesse & Noels 1993). Models in the grid are parametrized by  $X$  (initial hydrogen abundance),  $\alpha_{\text{ov}}$  (convective overshooting parameter),  $Z$  (metallicity), mass and age. At first instance, we fixed  $X = 0.70$  because slightly changing  $X$  is equivalent to slightly changing the metallicity  $Z$  for fitting the frequencies. We considered three values of  $\alpha_{\text{ov}}$ : 0.0, 0.1 and 0.2. We covered the mass range between 7 and  $13 M_{\odot}$  with a resolution of  $0.1 M_{\odot}$  and a metallicity range between 0.012 and 0.030 with a resolution of 0.002. In the age dimension we covered the whole main-sequence evolution from the zero-age main sequence (ZAMS) until the terminal-age main sequence (TAMS). For each stellar model, we have calculated the theoretical frequency spectrum of low-order p- and g-modes with a degree of the oscillation up to  $\ell = 4$  using a standard adiabatic code (Bouy et al. 1975).

From the observed frequency spectrum shown in Fig. 1 only the reliable frequencies corresponding to zonal modes ( $m = 0$ ) are suitable for a seismic analysis. Indeed, the theoretical frequency spectrum of non-rotating models should match the observed frequency spectrum of zonal modes in the first-order approximation, which is valid given the slow rotation of  $\nu$  Eri ( $v \sin i < 25 \text{ km s}^{-1}$ ; Aerts, Waelkens & De Pauw 1994; Paper II).

We selected the four frequencies  $f_1 = 5.7633 \text{ cd}^{-1}$  ( $= \nu_1$ ),  $f_2 = 5.637 \text{ cd}^{-1}$  ( $= \nu_4$ ),  $f_3 = 6.244 \text{ cd}^{-1}$  ( $= \nu_6$ ) and  $f_4 = 7.898 \text{ cd}^{-1}$  ( $= \nu_5$ ) from the observed frequency spectrum. We note that the  $\nu$ -notation between brackets corresponds with the frequency numbering presented in Paper III. In this paper we use the  $f$ -notation to distinguish the different frequency numbering adopted here for the sake of clarity. The selected frequencies are labelled in Fig. 1. Because these frequencies were clearly detected in both the photometric and spectroscopic data sets by all the different period analyses carried out independently by different researchers, we consider them as very reliable.

In Paper III the main mode  $f_1$  was clearly identified as a radial mode and  $f_2$  as well as  $f_3$  were found to be the central component of an  $\ell = 1$  triplet. The high-frequency mode  $f_4$  was also identified as a dipole mode but its azimuthal number  $m$  could not be derived. We perform the seismic modelling assuming that  $f_4$  is the central peak of the triplet. We show later that our results remain valid in the case when it would turn out that  $f_4$  is a side peak of the triplet.

Because a mode frequency not only depends on  $\ell$  and  $m$ , but also on the radial order  $n$ , we need to determine  $n$  of the selected frequencies before they can be fitted to theoretical frequencies. For an evolution sequence with  $X = 0.70$ ,  $\alpha_{\text{ov}} = 0.0$ ,  $Z = 0.020$  and  $M = 10 M_{\odot}$  there are three stages on the main sequence where a stellar model matches  $f_1$  and  $f_2$ , respectively, for the radial-order combinations  $(n_1, n_2) = (1, -1)$ ,  $(2, 1)$  and  $(3, 2)$ . An exploration of our grid of standard stellar models reveals that only the radial-order combination  $(n_1 = 1, n_2 = -1)$  leads to stellar models for which theoretical dipole modes are predicted in the close neighbourhood of  $f_3$  and  $f_4$ . Moreover, all these models identify the radial order of  $f_3$  and  $f_4$  as  $n_3 = 1$  and  $n_4 = 2$ , respectively. This result is in agreement with the identification made by Pamyatnykh et al. (2004) based partially on observational constraints.

Besides the matching of the four selected frequencies we take into account two additional observational constraints: the excitation of the pulsation modes, which we checked with a non-adiabatic pulsation code MAD (Dupret 2001), and the position in the Hertzsprung–Russell (HR) diagram relative to the error box that was derived in Paper III.

$\nu$  Eri is the first massive B-type star for which four independent observed frequencies can be used to perform a seismic analysis. The seismic modelling of, for example, EN(16) Lacertae (Thoul et al. 2003) as well as HD 129929 (Aerts et al. 2003; Dupret et al. 2004) was based on three pulsation modes. In both cases these frequencies were all well identified except for the third one of EN(16) Lacertae, for which the azimuthal number could not be derived. In the following sections we investigate how large the benefit is of having one more observed well-identified frequency in the case of  $\nu$  Eri.

## 3 FITTING TWO FREQUENCIES

We start the modelling with a fixed value for the parameters ( $X$ ,  $\alpha_{\text{ov}}$ ,  $Z$ ) and we calculate evolutionary tracks for different masses. On each evolutionary track, we select the model – thereby fixing the age – that fits  $f_1$  as the fundamental radial mode. For each of these stellar models, we compare the theoretically predicted frequency of

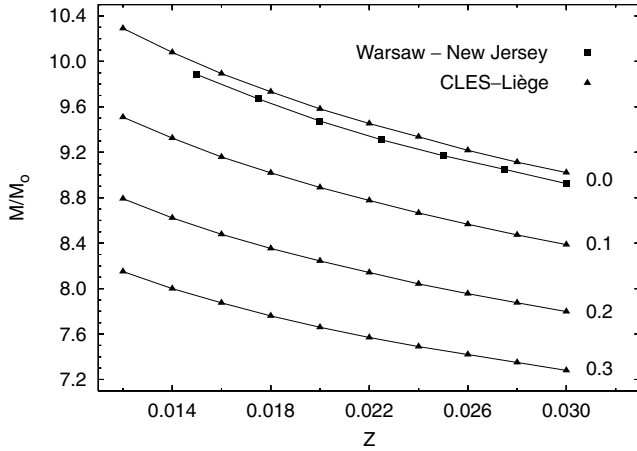


**Figure 2.** The  $M$ – $Z$  relations obtained by fitting  $f_1$  and  $f_2$  with the evolution code CLES (triangles) for four different ( $X = 0.70$ ,  $\alpha_{ov}$ ) sets. Each  $M$ – $Z$  relation is labelled with the  $\alpha_{ov}$  value for which it has been calculated. For comparison, the  $M$ – $Z$  relation obtained with the Warsaw–New Jersey code (squares) for the ( $X = 0.70$ ,  $\alpha_{ov} = 0.0$ ) set is also shown.

the  $\ell = 1$ ,  $g_1$  mode with  $f_2$ . Imposing a match gives us the mass  $M$ . So, by fitting two frequencies, we actually perform a mapping between the three-dimensional ( $X$ ,  $\alpha_{ov}$ ,  $Z$ ) parameter space and the two-dimensional ( $M$ , age) space.

At first instance we keep the parameters  $X$  and  $\alpha_{ov}$  constant and we vary the metallicity  $Z$  from 0.012 to 0.030 with steps of 0.002. For each such obtained ( $X$ ,  $\alpha_{ov}$ ,  $Z$ ) set, we perform the mapping. This yields an  $M$ – $Z$  relation for the considered ( $X$ ,  $\alpha_{ov}$ ) set. We calculated the  $M$ – $Z$  relations of the four sets ( $X = 0.70$ ,  $\alpha_{ov}$ ) with  $\alpha_{ov} = 0.0, 0.1, 0.2$  and  $0.3$ . The result is shown in Fig. 2. It follows that the mass decreases with an increase in the metallicity  $Z$  as well as an increase in the overshooting parameter  $\alpha_{ov}$ . Fig. 2 also shows the  $M$ – $Z$  relation obtained with the Warsaw–New Jersey code for the ( $X = 0.70$ ,  $\alpha_{ov} = 0.0$ ) set. The masses found with the Warsaw–New Jersey code are slightly lower, on average 1.15 per cent lower. No detailed comparison has been carried out so far in order to reveal the discrepancies between the different codes.

#### 4 FITTING THREE FREQUENCIES

As a subsequent step, we require the frequencies  $f_1$ ,  $f_2$  and  $f_3$  to be fitted by the models. This means that we perform a mapping between the two-dimensional ( $X$ ,  $\alpha_{ov}$ ) parameter space and the three-dimensional ( $Z$ ,  $M$ , age) space. Taking  $X = 0.70$  and no overshooting yields  $Z = 0.016$ ,  $M = 9.9 M_\odot$  and an age of 15.9 My. This stellar model also satisfies the two other observational constraints: the three modes are unstable and the position in the HR diagram is within the error box derived in Paper III. This immediately implies that there are many standard stellar models fulfilling all observational constraints when one imposes the fitting of  $f_1$ ,  $f_2$  and  $f_3$ . Indeed, the mapping can be performed for different values of  $\alpha_{ov}$ . Pamyatnykh et al. (2004) have discussed two such models in detail: one without overshooting and one with  $\alpha_{ov} = 0.1$ . We refer to that paper for details and omit to repeat similar results here.

Pamyatnykh et al. (2004) put an upper limit on the overshooting parameter at  $\alpha_{ov} = 0.12$  because standard stellar models with higher  $\alpha_{ov}$  values have an effective temperature below the lower observational bound they used. However, an updated better justified error box of  $\nu$  Eri’s position in the HR diagram was derived in Paper III, and this turns out to be somewhat larger than that used by

Pamyatnykh et al. (2004). Indeed, in Paper III it was shown that the temperature estimates obtained from different types of observations (photometry versus spectroscopy) are not the same. Therefore, we have chosen not to restrict the overshooting parameter on the basis of an error box. Our approach is a massive scan of the parameter space by means of our grid of stellar models without a priori confining our search. We will derive a value for  $\alpha_{ov}$  by imposing an exact fit of  $f_4$  and use the temperature estimate  $T_{\text{eff}} = 22\,900 \pm 1\,100$  K that was derived in Paper III to check a posteriori whether the resulting model lies significantly outside this error box or not.

#### 5 FITTING FOUR FREQUENCIES

By fitting  $f_1$  and  $f_2$  we carry out the mapping between the three-dimensional ( $X$ ,  $\alpha_{ov}$ ,  $Z$ ) parameter space and the two-dimensional ( $M$ , age) space for the points ( $X = 0.70$ ,  $\alpha_{ov}$ ,  $Z$ ) with  $\alpha_{ov} = 0.0, 0.1, 0.2$  and  $0.3$ , and  $Z$  values ranging from 0.012 to 0.030 with  $\Delta Z = 0.002$ . For each of these models we compare the theoretically predicted frequency values of the  $p_1$  and  $p_2$  dipole modes with  $f_3$  and  $f_4$ , respectively, in order to find the standard stellar model that fits all four frequencies. This comparison is shown in Fig. 3. It shows that  $f_3$  can be fitted, fairly independently of the value of  $\alpha_{ov}$ , by models with a metallicity of about 0.016, well in agreement with the results found by Pamyatnykh et al. (2004). An overshooting parameter higher than 0.3 is required however in order to fit  $f_4$ .

We recall from Section 2 our assumption that  $f_4$  is the central component of the triplet. However, the slow rotation of  $\nu$  Eri results in a close-frequency splitting (see also Fig. 1) so that the real  $p_2$  zonal mode can only have a slightly different frequency than  $f_4$ . It can then be deduced from Fig. 3 that, even when  $f_4$  turns out to be the left peak of the triplet, we still need an overshooting parameter of about 0.3 in order to fit the frequency of the central component.

The fitting of the four selected frequencies  $f_1$ ,  $f_2$ ,  $f_3$  and  $f_4$  leads to a mapping between the one-dimensional  $X$  parameter space and the four-dimensional ( $\alpha_{ov}$ ,  $Z$ ,  $M$ , age) space. For  $X = 0.70$ , this results in the values  $\alpha_{ov} = 0.313$ ,  $Z = 0.0155$ ,  $M = 7.83 M_\odot$  and age = 29.55 Myr.

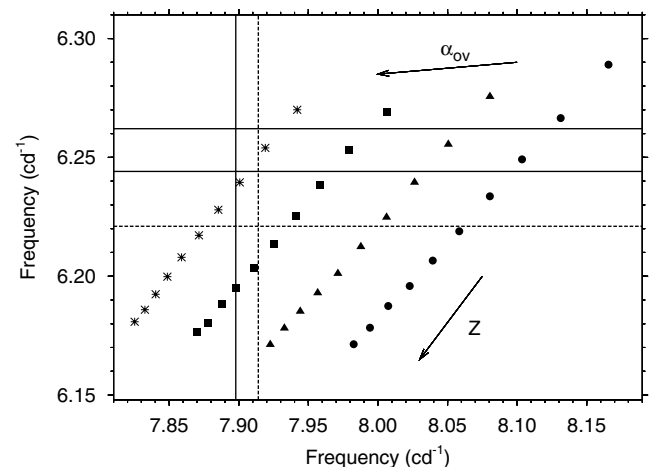


**Figure 3.** Frequency–frequency diagram in which the symbols mark the frequency values of the  $\ell = 1$ ,  $p_2$  (x-axis) and  $\ell = 1$ ,  $p_1$  mode (y-axis) as predicted by models that fit  $f_1$  and  $f_2$  for a given ( $\alpha_{ov}$ ,  $Z$ ) set. The four sequences correspond with  $\alpha_{ov} = 0.0$  (dots),  $0.1$  (triangles),  $0.2$  (squares) and  $0.3$  (asterisks). In each sequence the metallicity of the models ranges from 0.012 to 0.030 with steps of 0.002 in the shown direction. The solid and dashed lines denote the detected and suspected observed frequencies, respectively.

We note that the value of the overshooting parameter for  $\nu$  Eri derived with standard stellar models is rather high compared with the typical values taken for this parameter in the recent literature of oscillation studies (see Pamyatnykh 1999, for a discussion). However, high  $\alpha_{\text{ov}}$  values have been reported in studies of cluster fitting by, for example, Mermilliod & Maeder (1986), while Ribas, Jordi & Giménez (2000) studied eight early-type eclipsing binaries near or beyond the TAMS with masses ranging from 2 to 12  $M_{\odot}$  and found a systematic increase of  $\alpha_{\text{ov}}$  with the mass from 0.1 to 0.6. The latter value is needed to explain the evolved eclipsing binary V380 Cyg (Guinan et al. 2000). Schröder, Pols & Eggleton (1997) derived values slightly increasing from  $\alpha_{\text{ov}} \approx 0.24$  for 2.5  $M_{\odot}$  to  $\alpha_{\text{ov}} \approx 0.32$  for 6.5  $M_{\odot}$  based on the modelling of  $\zeta$  Aurigae binaries.

One should not exclude such high overshooting values without arguments. Here we provide two such arguments for  $\nu$  Eri. The standard stellar model calculated with CLES and fitting  $f_1$ ,  $f_2$ ,  $f_3$  and  $f_4$  has an effective temperature  $T_{\text{eff}} = 20\,235$  K, which is significantly outside the estimate  $T_{\text{eff}} = 22\,900 \pm 1100$  K derived in Paper III. Moreover, the result of a non-adiabatic analysis with MAD reveals that none of the four frequencies is predicted to be unstable. Therefore, we abandon the high-overshooting standard model. This implies that no standard stellar model matches all observational data of  $\nu$  Eri. We attempt to solve this problem by considering non-standard stellar models.

## 6 NON-STANDARD STELLAR MODELS

We consider none of the four modes being excited as the largest discrepancy between the standard stellar model fitting  $f_1$ ,  $f_2$ ,  $f_3$  and  $f_4$  and the observational data. Because the excitation of pulsation modes in B-type stars is due to the  $\kappa$ -mechanism active in the partial ionization zone of the heavy elements, especially of the iron group (Dziembowski & Pamyatnykh 1993; Gautschi & Saio 1993), we examine the effect of taking a different metal mixture.

Charpinet et al. (1996, 1997) and Fontaine et al. (2003) showed that the excitation of the pulsation modes in current models of sdB stars requires a local iron enrichment in the driving region, which may be the result of diffusion processes such as gravitational settling and radiative levitation. Pamyatnykh et al. (2004) followed this idea for  $\nu$  Eri by adopting an ad hoc iron enhancement in the driving zone. We have chosen to investigate the influence of uniform changes of the iron abundance throughout the stellar interior. Next to the standard solar mixture, we consider metal mixtures with an increase as well as a decrease in the relative number fraction of iron with a factor of 4. For each metal mixture we take three different values for

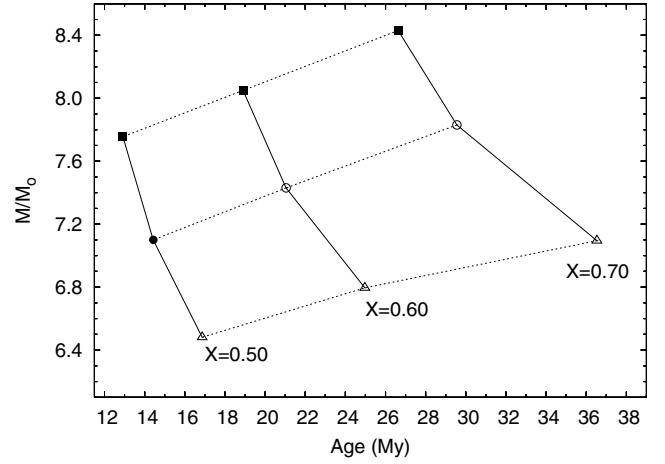


**Figure 4.** The values of the mass and the age are shown for the nine stellar models fitting  $f_1$ ,  $f_2$ ,  $f_3$  and  $f_4$  for different values of  $X$  and Fe. Models with the same  $X$  values are connected with full lines as indicated in the figure. The different mixtures Fe,  $4\text{ Fe}_{\odot}$  and  $1/4\text{ Fe}_{\odot}$  are denoted by circles, squares and triangles, respectively. Solid symbols correspond to models for which all four selected modes are unstable. This is not the case for models marked with open symbols.

$X$  (0.70, 0.60 and 0.50) in order to examine how low an  $X$  we must take in order to find a stellar model that satisfies all observational constraints. For each (Fe,  $X$ ) set we determine the values of  $\alpha_{\text{ov}}$ ,  $Z$ ,  $M$  and the age by fitting  $f_1$ ,  $f_2$ ,  $f_3$  and  $f_4$ . The results are listed in Table 1 and shown in Figs 4 and 5. A decrease in  $X$  results in lower values for  $\alpha_{\text{ov}}$ ,  $M$  and the age and higher ones for  $Z$ . A decrease in Fe lowers the mass  $M$  but raises the value of  $\alpha_{\text{ov}}$ ,  $Z$  and the age. As can be seen in Fig. 4, the derived masses are rather low – all below 8.5  $M_{\odot}$  for the considered (Fe,  $X$ ) sets – compared with typical values derived with standard stellar models. Fig. 5 shows that the values of the metallicity and the overshooting parameter are very sensitive to the considered changes in initial hydrogen abundance and relative number fraction of iron.

Subsequently, we check the instability of  $f_1$ ,  $f_2$ ,  $f_3$  and  $f_4$ . If a standard solar mixture is adopted, a value of  $X$  below 0.50 is needed in order to excite all four modes. Such a low  $X$  value is unrealistic from a physical point of view. If, however,  $X$  is fixed at 0.70, an increase in the relative number fraction of iron with a factor of 4 can also enable the excitation of all the selected frequencies. This is in agreement with what Pamyatnykh et al. (2004) found with

**Table 1.** Values of the stellar parameters  $\alpha_{\text{ov}}$ ,  $Z$ ,  $M$  and age derived by fitting  $f_1$ ,  $f_2$ ,  $f_3$  and  $f_4$  for models with different values of  $X$  and Fe. The values of other stellar parameters of the fitted models are also shown. The last column indicates whether the four selected modes are excited (+) or not (–). The most likely model from a physical point of view is indicated in *italics*.

Mixture	$X$	$\alpha_{\text{ov}}$	$Z$	$M/M_{\odot}$	Age (My)	$\log T_{\text{eff}}$	$\log L$	$R/R_{\odot}$	$\log g$	Excitation
$1/4\text{ Fe}_{\odot}$	0.70	0.44	0.0215	7.095	36.53	4.2792	3.584	5.715	3.775	–
	0.60	0.394	0.022	6.795	24.97	4.3103	3.695	5.625	3.770	–
	0.50	0.355	0.0235	6.481	16.87	4.3426	3.809	5.529	3.764	–
$\text{Fe}_{\odot}$	0.70	0.313	0.0155	7.83	29.55	4.3061	3.720	5.907	3.789	–
	0.60	0.287	0.0165	7.43	21.04	4.3331	3.812	5.799	3.782	–
	0.50	0.261	0.018	7.10	14.43	4.3649	3.925	5.705	3.776	+
$4\text{ Fe}_{\odot}$	<i>0.70</i>	<i>0.21</i>	<i>0.0115</i>	<i>8.43</i>	<i>26.63</i>	<i>4.3219</i>	<i>3.806</i>	<i>6.059</i>	<i>3.799</i>	+
	0.60	0.19	0.0125	8.05	18.90	4.3493	3.901	5.961	3.793	+
	0.50	0.157	0.0145	7.755	12.92	4.3799	4.012	5.884	3.788	+

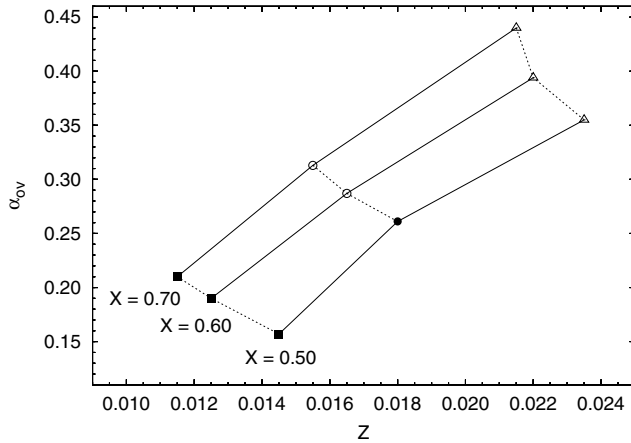


**Figure 5.** The values of the overshooting parameter and the metallicity are shown for the nine stellar models fitting  $f_1$ ,  $f_2$ ,  $f_3$  and  $f_4$  for different values of  $X$  and  $Fe$ . The adopted symbol convention is the same as in Fig. 4.

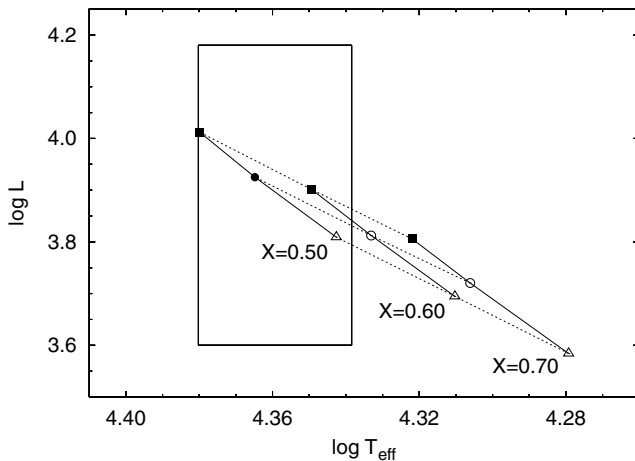


**Figure 6.** The position in the HR diagram is shown of nine stellar models fitting  $f_1$ ,  $f_2$ ,  $f_3$  and  $f_4$  for different  $(X, Fe)$  combinations. The rectangle represents the error box derived in Paper III. The adopted symbol convention is the same as in Fig. 4.

their ad hoc local increment of  $Fe$  in the driving zone in order to explain the driving of the mode with frequency  $f_4$ . It is apparent that an increase in the opacity caused by the excess  $Fe$  abundance is crucial to the driving mechanism of the oscillation modes. However, an overall change in the  $Fe$  fraction implies a very different stellar model compared to only a very local  $Fe$  increase in the driving zone.

Fig. 6 shows the position in the HR diagram of the nine stellar models that fit the four selected observed frequencies  $f_1$ ,  $f_2$ ,  $f_3$  and  $f_4$  for different  $(X, Fe)$  combinations. It shows that stellar models fitting  $f_1$ ,  $f_2$ ,  $f_3$  and  $f_4$  are within or closer to the error box if the relative number fraction of iron is increased or if the initial hydrogen abundance is decreased relative to their solar value. For stars in the solar neighbourhood, one expects  $X$  to lie in the range  $[0.68, 0.72]$ , and  $Fe$  not to be too different from the Sun, although this depends largely on the very local supernova history at the place of birth of  $\nu$  Eri. We can explain all the considered observational constraints, i.e. the frequency values, identifications and excitation of the four selected modes, for the model indicated in *italic* in Table 1, which is the most plausible solution from a physical point of view regarding

the hydrogen content. It turns out that this model is to the right of the observed error box of  $\nu$  Eri. However, increasing the  $Fe$  a little more, as well as decreasing  $X$  a little, will improve the position of the model with respect to the error box in the HR diagram. Such fine-tuning in position is, however, not useful at this stage because the error box was derived assuming standard models, an assumption which is inappropriate for  $\nu$  Eri. Moreover, also for the two other  $\beta$  Cephei stars for which seismic modelling was carried out in detail, a position to the right of the observational error box in the HR diagram was found (Aerts et al. 2003; Thoul et al. 2003; Dupret et al. 2004).

In Fig. 7 we compare the theoretical frequency spectra of the nine obtained models with the observed frequency spectrum. The theoretical frequency spectra are shown for modes with a degree up to  $\ell = 3$ . All observed frequencies (Papers I, II and III) are shown as vertical lines (solid and dashed lines for definitive and uncertain frequencies, respectively).

Because of the sparse theoretical frequency spectrum, we are able to identify unambiguously nearly all detected frequencies from photometry as well as from spectroscopy. As already mentioned in Section 2, the fitting of  $f_1$  and  $f_2$  as the radial fundamental mode and the  $\ell = 1$ ,  $g_1$  mode, respectively, leads to the identification of  $f_3$  and  $f_4$  as the  $\ell = 1$ ,  $p_1$  and  $\ell = 1$ ,  $p_2$  modes, respectively, which is in agreement with the photometric mode identification.

The frequency  $7.200 \text{ cd}^{-1}$  was clearly detected in the photometric data, but not in the spectra. Therefore, we did not include this frequency in the seismic modelling. The presence of a more uncertain peak at  $7.252 \text{ cd}^{-1}$  has also been reported in Paper I. Fig. 7 shows that this frequency, for which the corresponding mode could not be identified by the photometric mode identification (see Paper III), is nicely explained by an  $\ell = 2$ ,  $f$  mode. We point out that our modelling seems to identify the suspected photometric frequency  $7.252 \text{ cd}^{-1}$  as the central peak of the predicted quintuplet instead of the certain photometric frequency  $7.200 \text{ cd}^{-1}$ . The identification as an  $\ell = 2$ ,  $f$  mode is robust against the considered changes of  $X$  and the metal mixture.

The detailed frequency analysis on the line profiles of the Si III (455.3 nm) and Si III (456.8 nm) lines performed in Paper III revealed additional frequencies. On the one hand, the two frequencies  $5.512$  and  $5.889 \text{ cd}^{-1}$  were clearly detected. Although they can be explained as combination frequencies, arguments were given in Paper III in favour of them being genuine eigenfrequencies. On the other hand, two low-amplitude frequencies  $4.707$  and  $4.742 \text{ cd}^{-1}$  were also found. These four additional frequencies are also indicated in Fig. 7 as dashed vertical lines. The good overall agreement between the position of these four uncertain frequencies and the theoretical frequencies of the  $\ell = 3$  modes provides a strong case for the physical reality of (some of) these additional frequencies. Discriminating among the nine models is however very difficult because we do not know the exact position of the central component of the multiplets to which these additional observed frequencies belong. Moreover, we cannot exclude the theoretical frequencies of  $\ell = 4$  modes as possible candidates to match these additional frequencies.

## 7 DISCUSSION

We have performed a detailed seismic analysis of the  $\beta$  Cephei star  $\nu$  Eri with the Liège evolution and pulsation codes. We did not include diffusion in our computations. We prefer to exclude (radiative) diffusion before detailed theoretical calculations have been performed in the appropriate temperature and mass range (as far as we know, diffusion results are only available for A-type or later type stars). We hence did not change the physics of the models but

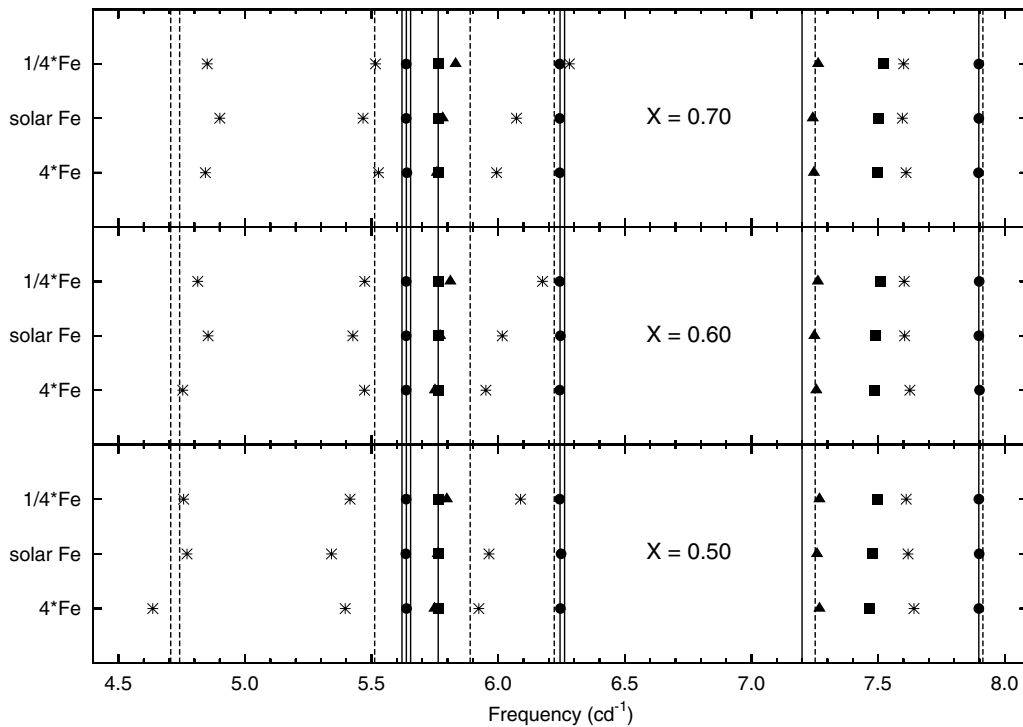


**Figure 7.** Comparison of the theoretical frequency spectrum of nine stellar models fitting  $f_1$ ,  $f_2$ ,  $f_3$  and  $f_4$  with all the observed frequencies (Papers I, II and III) in the range  $[4.4, 8.1] \text{ cd}^{-1}$ . The theoretical frequencies are denoted as squares, dots, triangles and asterisks for  $\ell = 0, 1, 2$  and  $3$  modes, respectively. The observed frequencies are indicated by vertical lines: certain frequencies (full lines) and uncertain frequencies (dashed lines). The nine stellar models, for which the theoretical frequency spectra are shown, have different  $X$  and Fe values. The theoretical spectra in the top, middle and bottom panels correspond to  $X = 0.70$ ,  $X = 0.60$  and  $X = 0.50$ , respectively. The three theoretical frequency spectra in each panel have been calculated for different mixtures as indicated on the y-axis.

we merely carried out a massive exploration of the stellar parameter space to fit the observational constraints.

We have shown the significance of considering four instead of three observed and identified frequencies in the case of  $\nu$  Eri. Matching three pulsation modes results in several standard stellar models that satisfy all other observational constraints. However, no standard stellar model fits and excites the four clearly detected pulsation modes  $f_1$ ,  $f_2$ ,  $f_3$  and  $f_4$ .

We subsequently calculated additional non-standard models fitting the four selected frequencies with different metal mixtures (relative number fraction of iron:  $\text{Fe}_{\odot}$ ,  $4 \text{ Fe}_{\odot}$  and  $1/4 \text{ Fe}_{\odot}$ ) and different  $X$  values (0.70, 0.60 and 0.50) to study the influence of these parameters on the excitation and the fitting of the four selected modes. A significant increase in Fe (a factor of 4 in relative number) or a significant decrease in  $X$  (a factor of almost 2) result in stellar models matching and exciting all four pulsation modes. These changes also bring the stellar model closer to or within the error box derived for the position in the HR diagram.

The calculated stellar models fitting  $f_1$ ,  $f_2$ ,  $f_3$  and  $f_4$  all yield the same identification of all observed frequencies, which is in full agreement with the photometric mode identification performed for some of them. We have also shown that most of the uncertain frequencies found in photometry or spectroscopy can be explained by theoretical  $\ell = 3$  modes in all models fitting the four selected frequencies. The uncertain nature of these observed frequencies, however, prevents further discrimination between the models fitting four frequencies for different metal mixtures and  $X$  values. The unambiguous detection of  $\ell = 3$  zonal modes would put even more constraints on the stellar models because of the significant changes

in the theoretical frequencies of the  $\ell = 3$  modes in the models fitting  $f_1$ ,  $f_2$ ,  $f_3$  and  $f_4$  (see Fig. 7). Another additional constraint could come from a more accurate determination of the effective temperature which is highly uncertain at present (Paper III).

Pamyatnykh et al. (2004) end up with quite different best models (more massive and younger) because they fitted only the three frequencies  $f_1$ ,  $f_2$  and  $f_3$  and restricted the overshooting parameter according to the uncertain error box based on photometric and parallax data (ignoring the spectral line profiles). They solved the excitation of the mode with frequency  $f_4$  by arguing that diffusive processes can probably induce a strong local enhancement of Fe in the driving zone, which would not change the global parameters of their best models fitting the three selected frequencies. The different outcome due to the different modelling procedures adopted by us and by Pamyatnykh et al. (2004) shows the great need of including diffusive processes in the theoretical structure model calculations for the temperature range of the  $\beta$  Cephei stars and of studying their effect on the calculated oscillation frequency values in full detail. We plan to tackle this point for  $\nu$  Eri in the near future.

$\nu$  Eri is the second  $\beta$  Cephei star for which evidence for non-rigid rotation was put forward. Aerts et al. (2003) and Dupret et al. (2004) used the frequency splittings of the  $\ell = 1$ ,  $p_1$  and  $\ell = 2$ ,  $g_1$  multiplets to rule out uniform rotation in the envelope of the  $\beta$  Cephei star HD 129929. In the case of  $\nu$  Eri, Pamyatnykh et al. (2004) inferred that the mean rotation rate in the  $\mu$ -gradient zone is about three times higher than in the envelope for their two standard models fitting the three observed frequencies  $f_1$ ,  $f_2$  and  $f_3$ . Their analysis was based on the  $\ell = 1$ ,  $g_1$  triplet and two components of the  $\ell = 1$ ,  $p_1$  triplet as observed in the photometric data

(Paper I). First, they predicted a value for the frequency of the third (left) component of the  $\ell = 1$ ,  $p_1$  triplet under the assumption that its asymmetry is caused by second-order effects of rotation with the same rate as for the  $\ell = 1$ ,  $g_1$  triplet. Secondly, they averaged out the asymmetry of both triplets and used the mean splittings to put constraints on the internal rotation. While the results of Pamyatnykh et al. (2004) for  $\nu$  Eri are remarkably similar to those of Aerts et al. (2003) and Dupret et al. (2004) for HD 129929, making it tempting to put forward that this may be a general result for slowly rotating stars in that position in the HR diagram, we are cautious of overinterpretation. Indeed, the frequency analyses of the different radial velocity time series (Papers II and III) all revealed a significant lower-frequency value for the left component of the  $\ell = 1$ ,  $p_1$  triplet. Therefore, the asymmetry within this triplet is much larger than that assumed in Pamyatnykh et al. (2004). We believe it is worthwhile to investigate the effect of this deviation from equidistance before refining the constraints on the internal rotation found by Pamyatnykh et al. (2004). Therefore, we plan to perform a future seismic analysis of  $\nu$  Eri based on stellar models which take the second-order effect of rotation into account, aiming for a model that fits and excites the four observed frequencies  $f_1$ ,  $f_2$ ,  $f_3$  and  $f_4$  and is able to reproduce the asymmetry of both observed triplets. Such modelling requires adaptation of our evolution and pulsation codes, which is beyond the scope of our current paper.

The goal of asteroseismology is the improvement of our current understanding of stellar physics. The observed global stellar parameters of stars are, however, not as well determined as for the Sun, particularly for massive stars. Such stars require the oscillation data to improve the global parameters first, before any significant tests of the presently available stellar structure theory can be undertaken.  $\nu$  Eri is a very rewarding star in this respect because it is the first  $\beta$  Cephei star for which enough observational constraints are available to show that standard stellar models are not able to satisfy them all. Given the thorough modelling that was already possible for  $\nu$  Eri on the basis of only a very limited number of frequencies, we are very hopeful for the future of asteroseismology of massive B-type stars.

## ACKNOWLEDGMENTS

We thank M.-A. Dupret for the use of the non-adiabatic pulsation code MAD. We are grateful to G. Handler, A. A. Pamyatnykh and W.A. Dziembowski for the discussions and the debates they held with us in the framework of the study of  $\nu$  Eri and for the provision

of data which we used in Fig. 2. We also thank J. De Ridder, A. Mazumdar, J. Daszynska, J. Montalbán, P.O. Bourge and A. Noels for the many fruitful meetings on the modelling of  $\nu$  Eri. MA is grateful to K. Lefever for a careful reading of this manuscript. This study was made possible thanks to support of the Research Fund K. U. Leuven under grant number GOA/2003/04.

## REFERENCES

- Aerts C., De Cat P., 2003, *Space Sci. Rev.*, 105, 453  
Aerts C., Waelkens C., De Pauw M., 1994, *A&A*, 286, 136  
Aerts C., Thoul A., Daszynska J., Scuflaire R., Waelkens C., Dupret M. A., Niemczura E., Noels A., 2003, *Sci.*, 300, 1926  
Aerts C. et al., 2004, *MNRAS*, 347, 463 (Paper II)  
Alexander D. R., Ferguson J. W., 1994, *ApJ*, 437, 879  
Boury A., Gabriel M., Noels A., Scuflaire R., Ledoux P., 1975, *A&A*, 41, 279  
Charpinet S., Fontaine G., Brassard P., Dorman B., 1996, *ApJ*, 471, L103  
Charpinet S., Fontaine G., Brassard P., Chayer P., Rogers F. J., Iglesias C. A., Dorman B., 1997, *ApJ*, 483, L123  
Christensen-Dalsgaard J., 2002, *Rev. Mod. Phys.*, 74, 1073  
Christensen-Dalsgaard J., Däppen W., 1992, *A&A Rev.*, 4, 267  
De Ridder J. et al., 2004, *MNRAS*, 351, 324 (Paper III)  
Dupret M.-A., 2001, *A&A*, 366, 166  
Dupret M.-A., Thoul A., Scuflaire R., Daszynska-Daszkiewicz J., Aerts C., Bourge P.-O., Waelkens C., Noels A., 2004, *A&A*, 415, 251  
Dziembowski W. A., Pamyatnykh A. A., 1993, *MNRAS*, 262, 204  
Fontaine G., Brassard P., Charpinet S., Green E. M., Chayer P., Billères M., Randall S. K., 2003, *ApJ*, 597, 518  
Gautschi A., Saio H., 1993, *MNRAS*, 262, 213  
Grevesse N., Noels A., 1993, in Pratz N., Vangioni E., Casse M., eds, *Origin and Evolution of the Elements*. Cambridge Univ. Press, Cambridge, p. 15  
Guinan E. F., Ribas I., Fitzpatrick E. L., Giménez Á., Jordi C., McCook G. P., Popper D. M., 2000, *ApJ*, 544, 409  
Handler G., Aerts C., 2002, *Commun. Asteroseismology*, 142, 20  
Handler G. et al., 2004, *MNRAS*, 347, 454 (Paper I)  
Iglesias C. A., Rogers F. J., 1996, *ApJ*, 464, 943  
Mermilliod J.-C., Maeder A., 1986, *A&A*, 158, 45  
Pamyatnykh A. A., 1999, *Acta Astron.*, 49, 119  
Pamyatnykh A. A., Handler G., Dziembowski W. A., 2004, *MNRAS*, 350, 1022  
Ribas I., Jordi C., Giménez Á., 2000, *MNRAS*, 318, L55  
Schröder K.-P., Pols O. R., Eggleton P. P., 1997, *MNRAS*, 285, 696  
Thoul A. et al., 2003, *A&A*, 406, 287

This paper has been typeset from a  $\text{\TeX}/\text{\LaTeX}$  file prepared by the author.